Stress Measurements in a Structural Component Using Magnetic Barkhausen Noise Analysis

Silverio F. SILVA JR.[1], Leonardo P. CARLECH[1], Miguel M. NETO[2]
Donizete A. ALENCAR[1], Guilherme G. BOTELHO[1]
[1] Centro de Desenvolvimento da Tecnologia Nuclear - CDTN, Belo Horizonte, Brasil
Phone: +55 31 3069 3289, Fax: +55 31 3069 3285
e-mail: silvasf@cdtn.br, daa@cdtn.br, lpc@cdtn.br
[2] Instituto de Pesquisas Energéticas e Nucleares – IPEN, São Paulo, Brasil
e-mail: mmattar@ipen.br

Abstract

The use of magnetic Barkhausen noise (MBN) analysis to perform measurements of applied stresses in structural components was studied. Experiments were conducted in a truss shape element, manufactured from samples of ASTM A 36 steel. Constant stress cantilever beams were instrumented with strain gage rosettes and used for test system calibration. The truss shape element was submitted to different loading conditions and the stresses induced were determined using simultaneously MBN analysis and three element strain gage rosettes. The results obtained have shown a good correlation between the two techniques in the interval of stresses evaluated.

Keywords: Barkhausen effect; stress analysis; non-destructive evaluation

1. Introduction

Magnetic methods have been considered as potential tools for non-destructive evaluation of ferromagnetic materials used for structural purposes. Magnetic Barkhausen noise (MBN) and magnetic hysteresis loop techniques have been used in applications such as creep evaluation, surface decarburization detection, deformation and fatigue studies [1-3]. Besides that, measurements of residual and applied stresses can be performed using MBN techniques [4-6]. However, measurements done with MBN techniques are affected by the combined effect of material microstructure, chemical composition and intensity of residual or applied stresses. For this reason, a study of a particular feature of a given material should be conducted under carefully controlled conditions, in order to maximize the influence of the desirable variable and minimize the others.

The Barkhausen effect originates from the interactions occurring between magnetic domain walls and pinning sites present into a ferromagnetic material during the magnetization process. Magnetic domain wall movement is affected by the presence of structural discontinuities such as grain boundaries, inclusions, precipitates, dislocations and mechanical stresses. During the magnetization, domain walls are pinned by these discontinuities. As the external magnetic field increases, the domain walls are released abruptly from the pinning sites, resulting in discrete changes in local magnetization, which can be detected as voltage pulses by a coil positioned in the surface of the material. A single voltage pulse produces an elementary Barkhausen event. The sum of all Barkhausen events during the magnetization is called magnetic Barkhausen noise [7].
Mechanical stresses influence the distribution of the domains and the dynamics of the domain walls' motion through the magnetoelastic interaction [8]. For materials that

present positive magnetostriction constant, compression stresses reduces the intensity of the Barkhausen noise, while tension stresses do increase it. For materials with negative magnetostriction constant, the behavior is the opposite. Usually, MBN versus stress presents a sigmoidal relationship. Below the yield point, for low tension or compression stress levels, MBN versus stress shows an almost linear relationship. For high tension or compression stress levels, saturation of MBN is verified [9]. The stress levels where the saturation occurs to depend on the material characteristics and can be determined during the test system calibration operations.

The experiments here described were performed in a specimen simulating a steel truss. The material used was the ASTM A 36 structural steel. Due to the number of variables that affect the MBN pattern, samples of the original steel plate, used in the construction of calibration and test specimens were taken. Their microstructure was characterized and mechanical properties determined. Furthermore, an experiment to determine the influence of the probe/specimen arrangement on the test results was performed. The information obtained was used to improve the methodology applied to the developed experiments.

2. Experimental methodology

2.1 Material characterization

ASTM A 36 steel chemical composition was determined using an ARL Optical Emission Spectrometer Model 3560 OES. The results are shown in Table 1.

Table 1 – Chemical composition of the ASTM A 36 steel plate

Chemical Element	C	Si	Mn	P	S	Fe
Content (%)	0.11	0.02	0.44	0.01	0.01	99.30

Tension and hardness tests were performed according to ASTM E 8M and ASTM E 92 standard practices respectively. The samples used in the tension tests were machined from specimens of the steel plate cut in the directions parallel and perpendicular to the rolling direction. The obtained results can be observed in Table 2.

Table 2 – Mechanical properties of the material studied

Test Direction	Yield stress σ_y (MPa)	Tensile strength σ_s (MPa)	Fracture stress σ_f (MPa)	Vickers hardness
Parallel to the rolling direction	291 ±15	396±8	253±6	116±5
Perpendicular to the rolling direction	304±5	399±5	273±2	

For microstructural analysis, metallographic samples representative of the cross section and the surface of the material were prepared, following conventional practices. Etching was performed using 2% NITAL solution. After that, average grain size of both samples was determined, using image processing software [10]. The microstructure of the samples can be observed in Fig. 1. The results obtained from the grain size measurements are shown in Table 3.

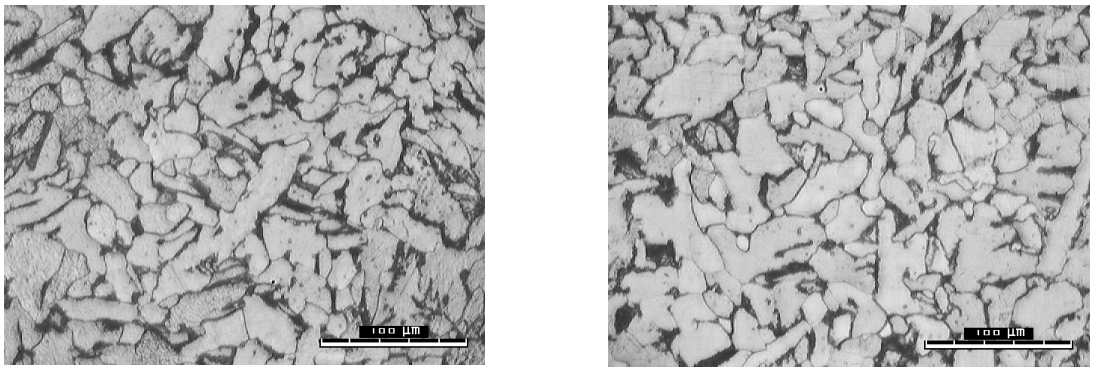

(a) (b)

Figure 1 - Microstructure of the ASTM A 36 steel samples: (a) sample representative of the materials cross section (ASTM A 36 F); (b) sample representative of the materials surface (ASTM A 36 D).

Table 3. Average grain size of the ASTM A 36 samples

Sample	Average grain diameter (µm)	Average grain width (µm)
ASTM A 36 D	9.9	14.3
ASTM A 36 F	9.7	11.2

2.2 Equipment and test parameters

A four channel Metalelektro Stresstest model 20.04 equipment and a uniaxial electromagnetic probe were used to obtain the magnetic Barkhausen noise data. Test excitation frequency was set to 100 Hz and the probe and was fed with a 1.57 Ampere excitation current. The magnetic Barkhausen noise was acquired using high-pass filters with frequencies cut-off frequencies of 500 Hz, 2 kHz, 8 kHz and 32 kHz.

2.3 Calibration specimens

Constant stress cantilever beams, similar to those used in ASTM E 251[11] were adopted as calibration test specimens. Despite of their more complex geometry, they present an important advantage in comparison to the constant cross section cantilever beams, usually used in the calibration phase. A constant stress cantilever beam is designed with a variable cross section. For this reason, the increasing in the bending moment along to the beam longitudinal axis, generated by a load applied at the beam extremity, is compensated by the increasing in the beam cross section. So, the stress

along to the beam longitudinal axis, in the same plane, remains constant, improving the calibration process. The thickness of the beams and the truss element is 6.35 mm.

Beams with the longitudinal axis parallel (beam A) and perpendicular (beam B) to the rolling direction of the material were cut, machined, submitted to a heat treatment for stress relief and instrumented with KFG-5-120-C1-11 KYOWA rosettes. An instrumented beam and the setup assembly used for the test system calibration can be observed in Fig. 2.

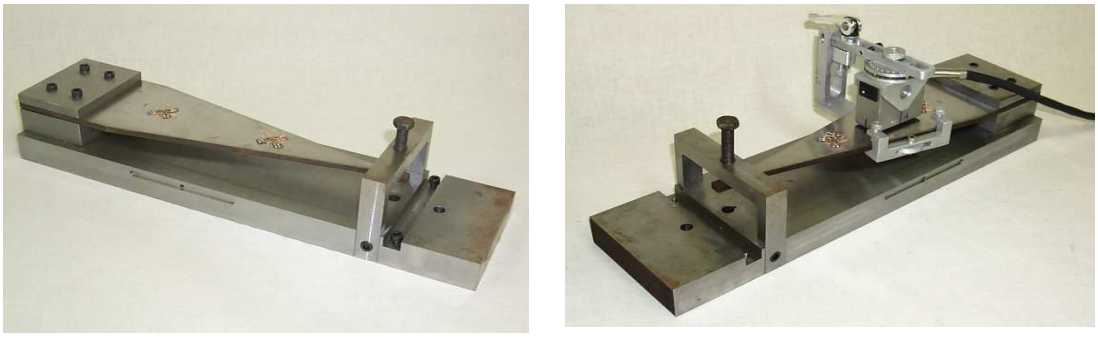

(a) (b)

Figure 2. Instrumented constant stress cantilever beams (a) and set-up used in the test system calibration.

During the calibration operation, the beams were submitted to different loads, applied at the beam extremity using the setup assembly shown in Fig. 2. The stresses generated at the beam surface, for each load condition, were determined from the measurements performed using the strain gage rosettes. At the same time, the magnetic Barkhausen noise, for each loading condition, was recorded. The applied loads were calculated to generate tension and compression stresses lower than 80% of the yield stress at the beams surface. The measurements were performed with the excitation magnetic field parallel to the longitudinal beam axis.

2.3 Test specimen

The test specimen was designed to simulate a truss shape. Additionally, it was submitted to the same stress-relief heat treatment applied to the constant stress cantilever beams. So, it was instrumented with KFG-5-120-C1-11-KYOWA strain gage rosettes, which were positioned at lateral and bottom surfaces.

The test specimen was prepared in such a way that the longitudinal axes of the lateral and bottom surfaces were parallel to the rolling direction of the ASTM A 36 steel plate used in the experiments.

Once attached to a suitable hydraulic press, six different loads were applied to it, in order to generate tension stresses in the horizontal surface (bottom element) and compression stresses in the lateral surface. The corresponding stresses were monitored by the rosettes, determining the value of the normal stresses induced in the truss, as well as the angle between them and the longitudinal axes of the truss.

At the same time, for each loading condition, MBN was recorded. The measurements were obtained applying the excitation magnetic field parallel to the longitudinal axis of the test specimen surface. The test specimen and the assembly used in the loading test can be observed in Fig. 3 and Fig. 4

Figure 3. Test specimen and electromagnetic probe.

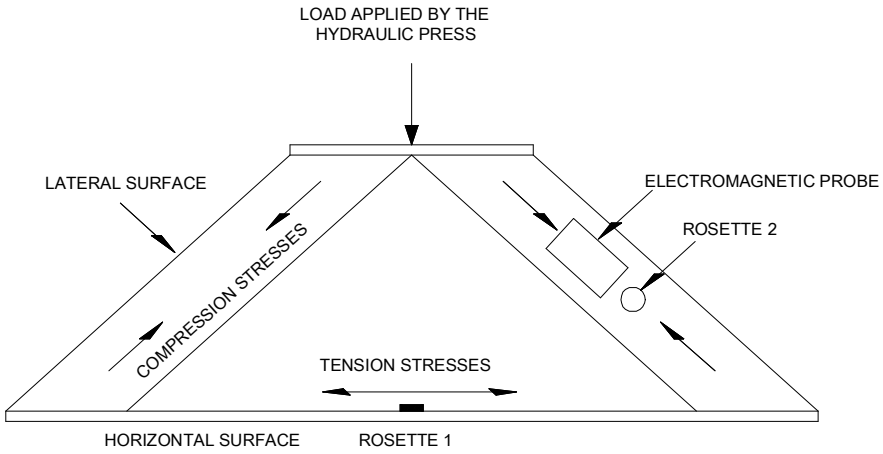

Figure 4. Assembly used in the loading test.

2.4 Lift-off effect

To verify how the probe to surface distance (lift-off) do affect the test results, a simple experiment was conducted. By means of a precise positioning system, RMS MBN values were registered for several probe to material surface distances.

3. Results and discussion

Curves corresponding to MBN values (mV_{RMS}) versus stress values (MPa) recorded in the calibration operation can be observed in Fig. 5.

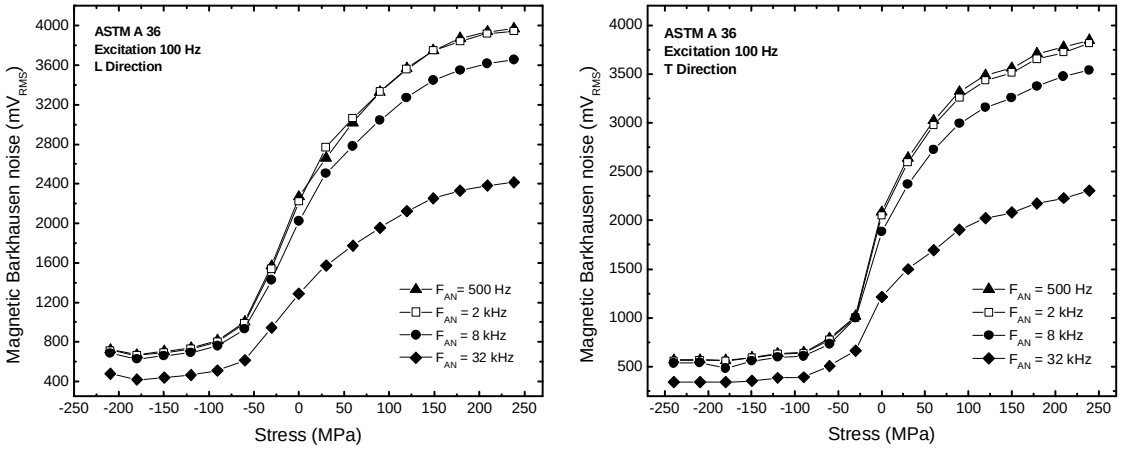

(a) (b)

Figure 5. Curves referent to the MBN RMS values versus stress levels. Constant stress beam with longitudinal axis parallel to the materials rolling direction – beam A (a) and perpendicular to the materials rolling direction beam B (b).

The MBN RMS values, measured in the rolling direction of the material (beam A) were larger than those measured in the perpendicular direction (beam B). For high tension stress levels, saturation of the MBN occurred. In the compression region, the saturation occurred for low levels of stresses. Between the regions where the saturation occurred, the measurements presented good sensitivity to stress changes.

The data presented in Fig. 5(a), referent to the measurements made in beam A were used to evaluate the stresses in the test specimen.

The results referent to the MBN RMS values versus stress values and the stress measurements performed by the strain gages rosettes in the test specimen, at different loading condition, can be observed in Fig. 6.

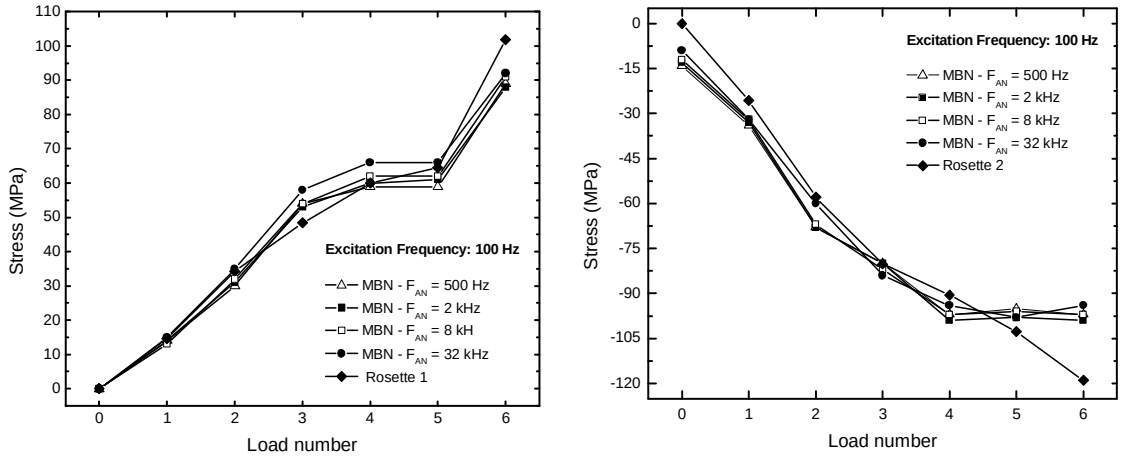

(a) (b)

Figure 6. Curves referent to the strees values determined in the loading test by MBN analysis and the strain gage rosettes. Tension stresses (a) and compression stresses (b).

Based on such results, it can be said that a good correlation between stresses values determined by the MBN analysis and those obtained with strain gage rosettes, was achieved. This behaviour can be observed in all analysis frequencies. The results suggest the applicability of MBN analysis as a reliable method to measure stresses in the range adopted in this experiment, for the steel used.

Moreover, it was possible to see that above ~ 100 MPa saturation of the MBN occurred for compression stresses. For tension stresses, no saturation was observed. These results are in accordance to the measurements performed in the calibration test specimens.

Finally, results concerning the experiment to check probe/material surface distance (lift-off) effects indicated a strong influence, as they can be observed in Fig. 6.

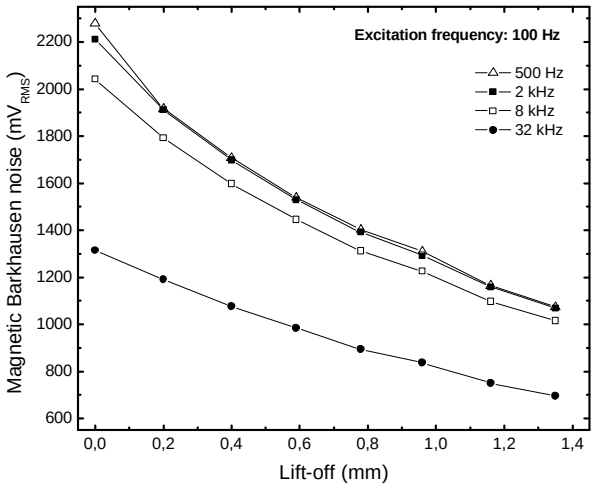

Figure 6. MBN RMS values versus lift-off curves. Excitation frequency of 100 Hz and analysis frequency of 500 Hz, 2 kHz, 8 kHz and 32 kHz.

Based on the test results, a special probe holder was developed to keep the probe in the same position at the calibration specimen surface/test specimen surface during all measurements.

4. Conclusions

The stress measurements performed using the MBN analysis have presented a good correlation with those determined using strain gage technology. Under tension conditions, the obtained results do indicate that the MBN analysis can be used for stress measurements in a large range. By other hand, in compression conditions, the test method is limited. Saturation occurred for low compression stress levels, about 100 MPa.

A strong dependence of the probe to material surface distance was also verified, making necessary to keep constant the probe/material arrangement during the calibration and the measurement operations.

In the next stages of this research, different materials will be used in the experiments, as well as test specimens designed to present uniform stress states under different loading conditions, in order to allow a more deep comprehension of the MBN behavior for stress measurements.

5. Acknowledgments

This work was funded by the “Fundação de Amparo à Pesquisa do Estado de Minas Gerais – FAPEMIG.

6. References

1. A. Mitra, J.N. Mohapatra, J. Swaminathan, M. Ghosh, A.K. Panda and R.N. Ghosh, 'Magnetic evaluation of creep in modified 9Cr–1Mo steel', Scripta Materialia Vol 57, pp 813–816, 2007.
2. R. Baldev, T. Jayakumar, V. Moorthy and S. Vaidyanathan, 'Characterization of Microstructures, Deformation, and Fatigue Damage in Different Steels Using Magnetic Barkhausen Emission Technique', Russian Journal of Nondestructive Testing, Vol 37, No 11, pp 789-798, 2001.
3. M. Blaow, J.T. Evans, B.A. Shaw, 'Surface decarburisation of steel detected by magnetic Barkhausen emission', Journal of Materials Science, Vol 40, pp 5517-5520, 2005.
4. M. Lindgren, T. Lepisto, 'On the stress vs. Barkhausen noise relation in a duplex stainless steel', NDT&International, Vol 37, pp 403-410, 2004.
5. G. Posgay, L. Imre, 'Stress Examination of Bridges Using Barkhausen Noise Measurement', 6TH European Conference on Nondestructive Testing, Nice, 1994.
6. N. Kuznetsov, I. Lyachenkov, A. Kuznetsov, V. Shaternikov, 'Estimation of Stresses in Pipelines by Magnetic Noise', In. 15TH World Conference on Nondestructive Testing, Rome, 2000.
7. S. Desvaux, M. Ourak, 'The evaluation of surface residual stress in aeronautic bearings using the Barkhausen noise effect', NDT&International, Vol 37, pp 9-17, 2004.
8. M.K. Devine, 'The magnetic Detection of Material Properties', JOM, pp 24-29, October 1992.
9. M. Blaow, J.T. Evans, B.A. Shaw, 'The effect of microstructure and applied stress on magnetic Barkhausen emission in induction hardened steel', Journal of Materials Science, Vol 42, pp 4364-4371, 2007.
10. L.C.M. Pinto, 'Quantikov – Um analisador microestrutural para o ambiente Windows', Tese de Doutorado. Universidade de São Paulo. 1996.
11. ASTM E 251. 'Standard Test Methods for Performance Characteristics of Metallic Bonded Resistance Strais Gages', AMERICAN SOCIETY FOR TESTING AND MATERIALS. USA, 2008.